LEAST-SQUARES MATCHING WITH ADVANCED GEOMETRIC TRANSFORMATION MODELS

F. Bethmann, *, T. Luhmann
Institute for Applied Photogrammetry and Geoinformatics, Jade University of Applied Sciences Oldenburg, Ofener Str. 16-19, D-26121 Oldenburg, Germany (folkmar.bethmann@jade-hs.de, thomas.luhmann@jade-hs.de)

Commission V, WG V/4

KEY WORDS: Least-Squares Matching, Image Matching, Accuracy

ABSTRACT:

The least-squares matching algorithm (LSM) for area-based image matching is a well known technique in photogrammetry and computer vision since more than two decades. Differences between two or more images can be modelled by estimating geometric and radiometric transformation functions within the functional model. Commonly the affine transformation is used as geometric transformation. Since this approach is not strict in terms of the projective imaging model, it is worthwhile to investigate alternative transformation models.
This paper presents an advanced least-squares matching algorithm that uses the projective transformation model and polynomial transformations to handle geometric distortions between the images. The projective approach is geometrically strict as long as object surface and image sensors are planes. The polynomial approach is supposed to be geometrically strict for plane image sensors and non-plane object surfaces. The possibility of this kind of expansions has been mentioned in several papers but up to now no publicly available investigation is known. First results of the new geometric model have been published by the authors in 2008, showing promising effects on non-planar object patches.

1. INTRODUCTION

Least squares matching (LSM) is a method for the geometric and radiometric matching of two or more image patches from a reference image (template) with respect to a search image. The method was developed in the beginning of the 1980ies. Förstner (1982) discussed the LSM approach for the one-dimensional case (applied to an image line) by integrating one translation parameter. Ackermann (1984), Pertl (1984) and Grün (1985) adopted the idea and enhanced it by additional geometric and radiometric parameters to the two-dimensional case with square or rectangular patches. All mentioned authors used an affine transformation as a linear geometric model. They have already stated that the applicability of affine transformation is restricted to small image patches if non-planar object surfaces appear. In the following years some interesting modifications of LSM have been published, e.g. the enhancement to multi-image adjustment with additional geometric constraints (Grün & Baltsavias 1988). More generalised approaches for object-oriented matching were developed by Wrobel (1987), Schneider (1990) and others. Since then he performance and practical usability has been demonstrated by many authors.

This paper presents an advanced least-squares matching algorithm that uses the projective transformation model and polynomial transformations to handle geometric distortions between the images. Within LSM the geometric relationship between two image planes (i.e. partially plane object surface) is strictly defined by the plane projective transformation (eq. (6)). As a consequence, the functional model becomes more complex since the model is not linear. If the surface consists of curvatures within the matching patch, polynomials of second or higher order (eq. (23)) can be applied.

In the following the functional models for the plane projective transformation and the second order polynomial transformation will be derived. Subsequently the geometric enhancement is investigated with respect to the matching accuracy.
In test 1 the two-dimensional matching accuracy is verified by means of synthetic image data. In test 2 the enhanced geometric functions have been implemented into a program for free-form surface measurement. A calibrated reference body is then measured providing a direct comparison of measured 3D data with respect to the calibrated surface.

2. THE FUNCTIONAL MODEL

Given two image functions of two patches of the same size:

$$g'(x',y') \quad \text{(image 1)}$$
$$g''(x'',y'') \quad \text{(image 2)}$$

The main idea for LSM is that image 1 can be projected into image 2 (in general image n) by geometric and radiometric transformation. Since the geometric model defines the functional relationship between both corresponding image patches, the coordinates of image 2 can be written as a function of the coordinates in image 1:

$$\begin{aligned} x'' &= f_x(x',y') \\ y'' &= f_y(x',y') \end{aligned} \quad (1)$$

Under consideration of the remaining noise functions $e'(x',y')$ and $e''(x'',y'')$ the geometric model between both image functions yields

* Corresponding author

$$g'(x',y')+e'(x',y')=g''(f_x(x',y'),f_y(x',y'))+e''(x'',y'') \quad (2)$$

Since the result of the transformation according to (1) is a non-integer number, the greyvalue g'' has to interpolated.
In general, functions f_x and f_y can be formed by arbitrary two-dimensional coordinate transformations. The here applied projective and polynomial transformations are described in detail in sections 2.1 and 2.2.
For the radiometric transformation usually a linear contrast stretching with two parameters is applied:

$$\begin{aligned} &g'(x',y')+e'(x',y') \\ &=r_0+r_1\cdot g''(f_x(x',y'),f_y(x',y'))+e''(x'',y'') \end{aligned} \quad (3)$$

The function is solved by least-squares approach where the square sum of greyvalue differences between the image patches is minimised. After substitution the noise functions to

$$v(x',y')=e'(x',y')-e''(x'',y'') \quad (4)$$

the observation equations are defined by

$$\begin{aligned} &l(x',y')+v(x'+y')= \\ &r_0+r_1\cdot g''(f_x(x',y'),f_y(x',y'))-g'(x',y') \end{aligned} \quad (5)$$

2.1 Projective transformation

Applying the plane projective transformation as the geometric model in (1), the following equations are used:

$$\begin{aligned} x''&=f_x(x',y')=\frac{a_0+a_1x'+a_2y'}{1+c_1x'+c_2y'} \\ y''&=f_y(x',y')=\frac{b_0+b_1x'+b_2y'}{1+c_1x'+c_2y'} \end{aligned} \quad (6)$$

Eight parameters are to be determined whereby a_0 and b_0 define the relative displacement between both image patches in x- und y-direction. Applying the transformation equations in (3), the linearised correction equation yield:

$$\begin{aligned} l(x',y')+v(x',y') &= r_0^0+r_1^0\cdot g''^0(f_x(x'^0,y'^0),f_y(x'^0,y'^0)) \\ &+\left(\frac{\partial g'}{\partial a_0}\right)^0 da_0+\left(\frac{\partial g'}{\partial a_1}\right)^0 da_1+\left(\frac{\partial g'}{\partial a_2}\right)^0 da_2 \\ &+\left(\frac{\partial g'}{\partial c_1}\right)^0 dc_1+\left(\frac{\partial g'}{\partial c_2}\right)^0 dc_2 \\ &+\left(\frac{\partial g'}{\partial b_0}\right)^0 db_0+\left(\frac{\partial g'}{\partial b_1}\right)^0 db_1+\left(\frac{\partial g'}{\partial b_2}\right)^0 db_2 \\ &+\left(\frac{\partial g'}{\partial c_1}\right)^0 dc_1+\left(\frac{\partial g'}{\partial c_2}\right)^0 dc_2 \\ &+\left(\frac{\partial g'}{\partial r_0}\right)^0 dr_0+\left(\frac{\partial g'}{\partial r_1}\right)^0 dr-g'(x',y')_1 \end{aligned} \quad (7)$$

It has to be pointed out that the differential quotients for parameters c_1 and c_2 appear twice, since partial derivatives are built in each f_x and f_y. They can be combined later (eq. (21) and (22)).
The partial derivatives of the geometric parameters are formed by the derivatives of the outer function (image function) and the inner function (geometric transformation). The derivatives of the outer function correspond to the image gradients

$$\begin{aligned} g_x&=\frac{\partial g''^0(x'',y'')}{\partial x''} \\ g_y&=\frac{\partial g''^0(x'',y'')}{\partial y''} \end{aligned} \quad (8)$$

The greyvalue gradients can be determined by suitable operators, e.g. Roberts gradient.
In particular the differential quotients of all ten unknowns are given by:

$$\frac{\partial g'}{\partial a_0}=r_1\cdot g_x\cdot\frac{1}{1+c_1x'+c_2y'} \quad (9)$$

$$\frac{\partial g'}{\partial a_2}=r_1\cdot g_x\cdot y'\cdot\frac{1}{1+c_1x'+c_2y'} \quad (10)$$

$$\frac{\partial g'}{\partial c_2}=-r_1\cdot g_x\cdot y'\cdot\frac{a_0+a_1x'+a_2y'}{(1+c_1x'+c_2y')^2} \quad (11)$$

$$\frac{\partial g'}{\partial b_1}=r_1\cdot g_y\cdot x'\cdot\frac{1}{1+c_1x'+c_2y'} \quad (12)$$

$$\frac{\partial g'}{\partial c_1}=-r_1\cdot g_y\cdot x'\cdot\frac{b_0+b_1x'+b_2y'}{(1+c_1x'+c_2y')^2} \quad (13)$$

$$\frac{\partial g'}{\partial r_0}=1 \quad (14)$$

$$\frac{\partial g'}{\partial a_1}=r_1\cdot g_x\cdot x'\cdot\frac{1}{1+c_1x'+c_2y'} \quad (15)$$

$$\frac{\partial g'}{\partial c_1}=-r_1\cdot g_x\cdot x'\cdot\frac{a_0+a_1x'+a_2y'}{(1+c_1x'+c_2y')^2} \quad (16)$$

$$\frac{\partial g'}{\partial b_0}=r_1\cdot g_y\cdot\frac{1}{1+c_1x'+c_2y'} \quad (17)$$

$$\frac{\partial g'}{\partial b_2}=r_1\cdot g_y\cdot y'\cdot\frac{1}{1+c_1x'+c_2y'} \quad (18)$$

$$\frac{\partial g'}{\partial c_2}=-r_1\cdot g_y\cdot y'\cdot\frac{b_0+b_1x'+b_2y'}{(1+c_1x'+c_2y')^2} \quad (19)$$

$$\frac{\partial g'}{\partial r_1}=g'^0(x',y') \quad (20)$$

Applying the differential quotients in (7), equations (16) and (13) as well as (11) and (19) can be combined:

$$\frac{\partial g'}{\partial c_1}=-r_1\cdot x'\left(g_x\cdot\frac{a_0+a_1x'+a_2y'}{(1+c_1x'+c_2y')^2}+g_y\cdot\frac{b_0+b_1x'+b_2y'}{(1+c_1x'+c_2y')^2}\right) \quad (21)$$

$$\frac{\partial g'}{\partial c_2}=-r_1\cdot y'\left(g_x\cdot\frac{a_0+a_1x'+a_2y'}{(1+c_1x'+c_2y')^2}+g_y\cdot\frac{b_0+b_1x'+b_2y'}{(1+c_1x'+c_2y')^2}\right) \quad (22)$$

2.2 Polynomial transformation

Applying the polynomial transformation as the geometric model in (1), the following equations are used:

$$x'' = f_x(x', y') = \sum_{j=0}^{n}\sum_{i=0}^{j} a_{ji} \cdot x'^{j-i} \cdot y'^{i}$$
$$y'' = f_y(x', y') = \sum_{j=0}^{n}\sum_{i=0}^{j} b_{ji} \cdot x'^{j-i} \cdot y'^{i} \quad (23)$$

Parameter n defines the polynomial order and will be set to n=2. Consequently, the 12 parameters a_{00},a_{10},a_{11},a_{20},a_{21},a_{22}, b_{00},b_{10},b_{11},b_{20},b_{21},b_{22} are to be determined as unknowns. The coefficients a_{00} and b_{00} define the relative displacement between both image patches in x- und y-direction.
In analogy to (7) linearised correction equation must be formed. The differential quotients yield:

$$\frac{\partial g'}{\partial a_{00}} = r_1 \cdot g_x \cdot 1 \quad (24)$$
$$\frac{\partial g'}{\partial a_{10}} = r_1 \cdot g_x \cdot x' \quad (25)$$
$$\frac{\partial g'}{\partial a_{11}} = r_1 \cdot g_x \cdot y' \quad (26)$$
$$\frac{\partial g'}{\partial a_{20}} = r_1 \cdot g_x \cdot x'^2 \quad (27)$$
$$\frac{\partial g'}{\partial a_{21}} = r_1 \cdot g_x \cdot x' \cdot y' \quad (28)$$
$$\frac{\partial g'}{\partial a_{22}} = r_1 \cdot g_x \cdot y'^2 \quad (29)$$
$$\frac{\partial g'}{\partial b_{00}} = r_1 \cdot g_y \cdot 1 \quad (30)$$
$$\frac{\partial g'}{\partial b_{10}} = r_1 \cdot g_y \cdot x' \quad (31)$$
$$\frac{\partial g'}{\partial b_{11}} = r_1 \cdot g_y \cdot y' \quad (32)$$
$$\frac{\partial g'}{\partial b_{20}} = r_1 \cdot g_y \cdot x'^2 \quad (33)$$
$$\frac{\partial g'}{\partial b_{21}} = r_1 \cdot g_y \cdot x' \cdot y' \quad (34)$$
$$\frac{\partial g'}{\partial b_{22}} = r_1 \cdot g_y \cdot y'^2 \quad (35)$$
$$\frac{\partial g'}{\partial r_0} = 1 \quad (36)$$
$$\frac{\partial g'}{\partial r_1} = g'^0(x', y') \quad (37)$$

Now the equation system of linearised correction equations can be formed. The vector of unknowns $\hat{\mathbf{x}}$ contains the corrections of the transformation parameters, the design matrix **A** contains the differential quotients, the observation corrections are stored in vector **v** and the greyvalue differences are kept in vector **l**. The following equation system must be solved:

$$\underset{n,1}{\mathbf{l}} + \underset{n,1}{\mathbf{v}} = \underset{n,u}{\mathbf{A}} \cdot \underset{u.n}{\hat{\mathbf{x}}} \quad (38)$$

where

n:	number of observations (= number of pixels in reference image)
u	number of unknowns (8 or 12 geometry parameters and 2 radiometry parameters)

Least squares adjustment according to L2 norm yields:

$$\hat{\mathbf{x}} = (\mathbf{A}^T\mathbf{PA})^{-1} \cdot (\mathbf{A}^T\mathbf{Pl}) \quad (39)$$

Using identical weights for all observations, the weight matrix **P** becomes the identity matrix. In some cases it might be useful to use individual weights, for instance if particular parts of the reference image are of higher importance for the matching, e.g. the centre of the window. Some of these weighting functions have been discussed by Piechel (1991).

Equation (39) will be solved iteratively. Since some of the differential quotients contain unknowns, the **A** matrix must be set up in each iteration.

3. INVESTIGATIONS

Two different test scenarios are described in the following section. In test 1 the accuracy of calculated image coordinates after matching is investigated, hence the quality of parameters a0 and b0. For this purpose synthetic image data is created so that nominal values for the geometric transformation parameters are known. In this way the effectiveness of the enhanced models can be investigated with respect to arbitrary geometric transformations, limitations, required initial values and other input values.

For test 2 the enhanced functions have been implemented into our program system PISA (**P**hotogrammetric **I**mage **S**equence **A**nalysis) which is used for free-form surface reconstruction in dynamic scenes. For accuracy assessment a 3D surface reference body has been developed which has been calibrated by a CMM with an accuracy of about 10µm (Fig. 7). Based on calibrated and oriented stereo cameras the surface is measured by different matching approaches and compared to the reference surface. In this manner absolute quantitative accuracy figures can be determined. In addition, by means of colour coded deviation maps systematic errors and matching outliers can easily be visualised. First experiences with the 3D reference body and the PISA package have been published by Luhmann et al. (2008) and Bethmann et al. (2009).

If least squares matching is applied a number of different aspects affect the final result significantly:

- greyvalue distribution of image functions (texture)
- patch size of template (reference window)
- amount of geometric distortion between both images
- quality of initial values, especially for shift parameters
- selection of transformation functions for matching

The main objective of the following investigations is the better understanding of the effect on matching quality for different geometric approaches. For sake of comparison only the geometric transformation function is modified in the following tests.

3.1 Test 1

For the first test an image is modified by projective and polynomial transformation with given parameters (Fig. 1):

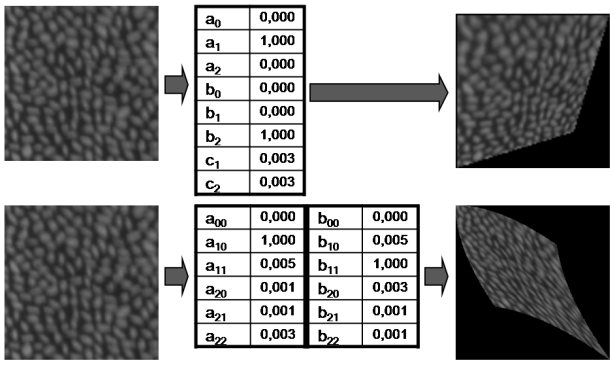

Fig. 1: Generation of synthetic image data (projective and polynomial)

Subsequently both image pairs are matched by LSM using affine, projective and polynomial transformation (template size: 20 x 20 pixel). The following diagrams show the differences between nominal and measured data for the shift parameters a_0 and b_0 after 15 iterations. Fig. 2 shows the results for the image pair that has been resampled by projective transformation.

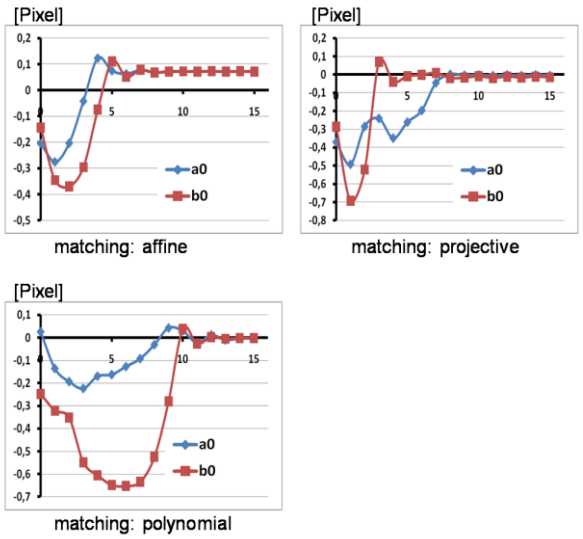

Fig. 2: Deviations of shift parameters for the projectively distorted image pair

Using the affine transformation a systematic offset of about 1/10 pixel remains after 7 iterations. As expected, using the projective transformation the nominal values are achieved after 8 iterations. If the polynomial function is used the nominal values are also obtained, yet after 11 iterations. It can be concluded that the polynomial approach is able to handle projective distortions. Since the polynomial function can not be derived from the projective transformation and vice versa, the latter result is of major importance.

Fig. 3 shows the differences between nominal and measured data for the shift parameters a_0 and b_0 after matching of the image pair that has been resampled by polynomial transformation:

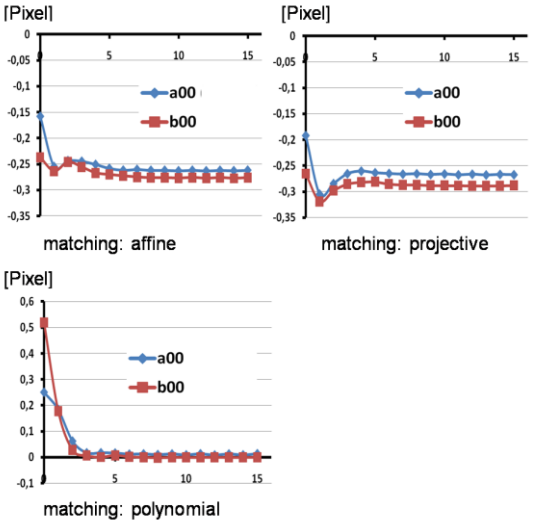

Fig. 3: Deviations of shift parameters for the polynomially distorted image pair

The results show that affine and projective transformation yield to similar systematic errors in the order of 1/4 to 1/3 pixel. Again as expected, the polynomial approach leads to nominal values.

The tests have been repeated for further image pairs that are similar to the images shown in Fig. 1 but different with respect to the amount of the geometric distortions. Fig. 4 gives an impression about applied image deformations. Applying the advanced geometric models to these image pairs yields to almost the same results as they are described above.

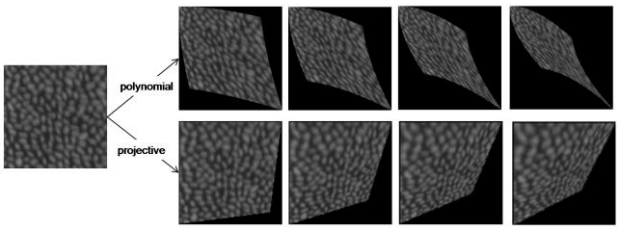

Fig. 4: Synthetic image data (projective and polynomial) with different geometric distortions

Summarising it can be stated that only the use of the polynomial approach yields to the correct match of both image examples.

For both approaches (projective, polynomial) the correlations between the estimated unknowns have been investigated. For the projective model partially high correlations (>0.9) can be observed, in particular for parameters c_1, c_2 and parameters $a_{1\text{-}2}$ and $b_{1\text{-}2}$. (see Fig. 5**:**). Further investigations will concentrate on significance and automated elimination of parameters. Using the polynomial model correlations of >0.7 do not exist in any case (see Fig. 5**:**).

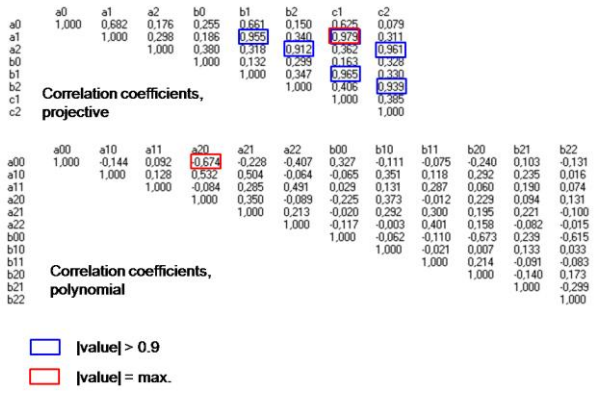

Fig. 5: Correlation coefficients (projective, polynomial)

3.2 Test 2

For test 2 the 3D reference body of Fig. 7 is observed by two high-speed cameras MiniVis Eco 2 (1.3 Mega pixel, focal length c = 12.5 mm, object distance h = 700 mm, stereo base b = 600 mm).

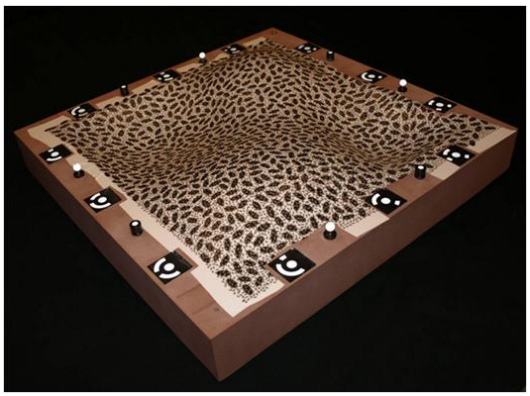

Fig. 6: 3D reference body

Both cameras are calibrated previously and oriented by means of coded targets that are attached to the reference body. The stereo images are processed with PISA using three different geometric approaches (affine, projective, polynomial). For matching a patch size of 25 x 25 pixel (equivalent to 18 x 18 mm in object space) has been used which adapts to the texture resolution of the object surface.

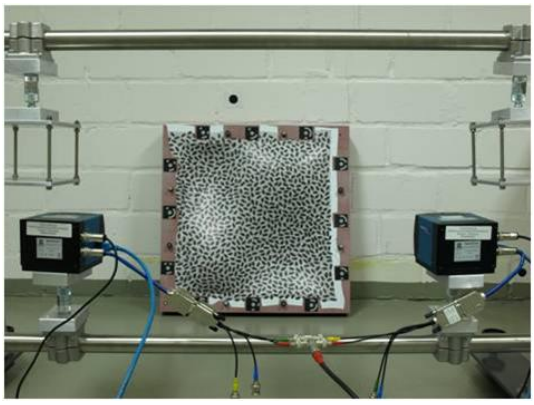

Fig. 7: Experimental set-up with MiniVis cameras

The object surface is measured with a point spacing of about 3 mm yielding about 23000 points. Fig. 8 shows the comparison of measured points against calibrated data.

Affine and projective approach lead to very similar results, thus only projective results are displayed. It can clearly be seen that systematic errors appear for the "valleys" (positive deviations) and for the "hills" (negative deviations). The same effect is visible for the histograms of deviations in Fig. 8 The error distribution shows a wide shape which is not normally distributed. Only in areas that are relatively flat the deviations lie within an interval of about ±0.050 mm. Table 1 summarizes the achieved accuracies.

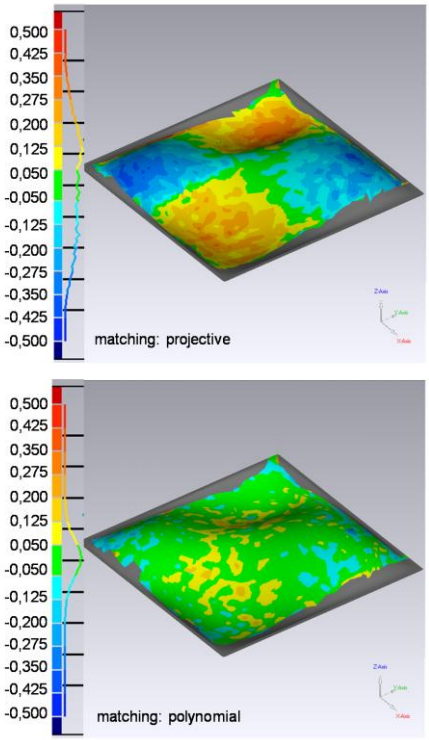

Fig. 8: 3D deviations after matching (left: projective; right: polynomial)

Using the polynomial approach no systematic errors are visible. The percentage of point within the interval of ±0.050 mm rises from 15% to 65%, while the mean square error drops from 0.178 mm to 0.056 mm (see Table 1).

	affine	**projective**	**polynomial**
RMS [mm]	0.222	0.178	0.056
points within ± 0.050mm	11%	15%	65%
points within ± 0.100mm	30%	40%	95%

Table 1: RMS values and number of points within ±0.050 mm and ±0.100 mm

In conjunction with this test the above mentioned patch size for matching has to be discussed. Additional tests have shown the

remaining systematic errors become less for affine and projective transformations with smaller patch sizes.

In practice the limiting factors for minimising patch sizes are, on the one hand, the selected transformation model and hence the number of estimated unknowns. On the other hand, object texture and imaging resolution play an important role for selectable patch sizes. Therefore, the theoretically miminum patch size can not be used. In addition, even with minimum patch sizes systematic deviation remain in the measured data. For applications with highest accuracy specifications the type of geometric model, the resolution of texture and imaging devices and the maximum curvature of the object surface have be taken into account in order to select the most useful configuration.

4. SUMMARY

The article presents two enhancements for least squares matching concerning the geometric transformation model. The approaches of plane projective transformation and of polynomial transformation have been investigated.

Within two test series it could be shown that affine and projective transformations yield systematic errors for the measured coordinates which depend on the selected matching patch size. In addition it could be demonstrated that the polynomial approach allows for a high accurate reconstruction of curved surfaces. In all tests the polynomial transformation generates result without remaining systematic errors whereby the results are, within reasonable limits, independent of the selected patch size.

5. REFERENCES

Ackermann, F. (1984): *Digital image correlation: performance and potential in photogrammetry*. Photogrammetric Record 11 (64), S. 429-439.

Bethmann, F., Herd, B., Luhmann, T., Ohm, J. (2009): *3D-Erfassung von Freiformflächen aus Bildsequenzen unter Berücksichtigung von Störobjekten*. In: Publikationen der Deutschen Gesellschaft für Photogrammetrie, Fernerkundung und Geoinformation e.V., Band 18, S. 303-315.

Foerstner, W. (1982): *On the geometric precision of digital correlation*. International Archives of Photogrammetry and Remote Sensing, 24 (3): S. 176-189.

Gruen, A. W. (1985): *Adaptive least-squares correlation – a powerful image matching technique*. South African Journal of Photogrammetry, Remote Sensing and Cartography, 14 (3): S. 175-187.

Gruen, A. W., Baltsavias, E. P., (1988): *Geometrically constrained multiphoto matching*. Photogrammetric Engineering and Remote Sensing, 54 (5): S. 633 – 641.

Luhmann, T., Bethmann, F., Herd. B., Ohm, J. (2008): *Comparison and Verification of Optical 3-D Surface Measurement Systems*. International Archives for Photogrammetry and Remote Sensing, Vol. 37, Part 5B, Beijing, pp. 51-56.

Pertl, A. (1984): *Digital image correlation with the analytical plotter Planicomp C-100*. International Archives of Photogrammetry and Remote Sensing 25 (3B), S. 874-882.

Piechel, J. (1991): *Qualität der automatischen Höhenmessung in Stereobildern durch flächenbasierte Kernlinienkorrelation*. Deutsche Geodätische Kommission bei der Bayrischen Akademie der Wissenschaften, Dissertationen, Reihe C, Heft Nr. 376.

Schneider, C. T. (1991): *Objektgestützte Mehrbildzuordnung*. Dissertation, Deutsche Geodätische Kommission, Reihe C, Nr. 375.

Wrobel, B. (1987). *Digitale Bildzuordnung durch Facetten mit Hilfe von Objektraummodellen*. Bildmessung und Luftbildwesen (BuL), Band 55, Heft 3, S. 93-101.